



**Ocean mediation of tropospheric response to reflecting and absorbing aerosols**

Y. Xu and S.-P. Xie

# Ocean mediation of tropospheric response to reflecting and absorbing aerosols

Y. Xu<sup>1</sup> and S.-P. Xie<sup>2</sup>

<sup>1</sup>National Center for Atmospheric Research, Boulder, CO 80303, USA

<sup>2</sup>Scripps Institution of Oceanography, University of California, San Diego, La Jolla, CA 92093, USA

Received: 24 January 2015 – Accepted: 13 February 2015 – Published: 25 February 2015

Correspondence to: Y. Xu (yangyang@ucar.edu)

Published by Copernicus Publications on behalf of the European Geosciences Union.

Title Page

Abstract

Introduction

Conclusions

References

Tables

Figures



Back

Close

Full Screen / Esc

Printer-friendly Version

Interactive Discussion



## Abstract

Radiative forcing by reflecting (e.g., sulfate, SO<sub>4</sub>) and absorbing (e.g., black carbon, BC) aerosols is distinct: the former cools the planet by reducing solar radiation at the top of the atmosphere and the surface, without largely affecting the atmospheric column, while the latter heats the atmosphere directly. Despite the fundamental difference in forcing, here we show that the structure of the tropospheric response is remarkably similar between the two types of aerosols, featuring a deep vertical structure of temperature change (of opposite sign) in the Northern Hemisphere (NH) mid-latitudes. The deep temperature structure is anchored by the slow response of the ocean, as large meridional sea surface temperature (SST) gradient drives an anomalous inter-hemispheric Hadley circulation in the tropics and induces atmospheric eddy adjustments in the NH mid-latitudes. The robust tropospheric response is unique to aerosol forcing and absent in the CO<sub>2</sub> response, which can be exploited for climate change attribution. The tropospheric warming in response to projected future decline in reflecting aerosols poses additional threats to the stability of mountain glaciers in NH.

## 1 Introduction

Greenhouse gas-induced global warming is partially masked (Ramanathan and Feng, 2008) by the accompanying increase in anthropogenic aerosols (Smith et al., 2011). Relative contribution of aerosol masking effect on global temperature is hard to quantify for the following reasons: (a) some aerosols (e.g., black carbon (BC) and organics absorb sunlight and heat the planet (Bond et al., 2013) and (b) aerosol microphysical effects on clouds are complex (Rosenfeld et al., 2013). Many ongoing efforts aim to reduce uncertainties in radiative forcing (Xu et al., 2013) and quantify the surface temperature response to aerosols (Levy et al., 2013). The atmospheric circulation response to reflecting aerosols has important effects on regional climate (e.g., the Indian monsoon, Bollasina et al., 2011) and hydrological cycle (Shindell et al., 2012; Hwang

ACPD

15, 5537–5552, 2015

## Ocean mediation of tropospheric response to reflecting and absorbing aerosols

Y. Xu and S.-P. Xie

Title Page

Abstract

Introduction

Conclusions

References

Tables

Figures

◀

▶

◀

▶

Back

Close

Full Screen / Esc

Printer-friendly Version

Interactive Discussion

## Ocean mediation of tropospheric response to reflecting and absorbing aerosols

Y. Xu and S.-P. Xie

Title Page

Abstract

Introduction

Conclusions

References

Tables

Figures

◀

▶

◀

▶

Back

Close

Full Screen / Esc

Printer-friendly Version

Interactive Discussion

et al., 2013). Much attention has been given to absorbing aerosols for the direct atmospheric heating effect, including BC (Meehl et al., 2010) and dusts (Vinoj et al., 2014). It is often argued that, by heating directly the atmosphere, absorbing aerosols can greatly perturb the atmospheric temperature structure, causing changes in stability and circulation (Lau et al., 2006). The atmospheric response, especially that of clouds, is hypothesized to be sensitive to the vertical profile of atmospheric heating (Koch and Del Genio, 2010). Reflecting aerosols, however, are considered less effective in driving large-scale circulation changes (Allen et al., 2012).

While previous studies focused on radiative forcing and climate impacts of aerosols on surface temperature and precipitation (Table S1 in the Supplement), few looked at the tropospheric response. Using climate model simulations, we show that the atmospheric responses (temperature and circulation) to reflecting and absorbing aerosols are surprisingly similar in structure (aside from a sign difference). Both responses feature a deep vertical temperature structure in the Northern Hemisphere (NH) mid-latitudes, with a shift in the westerly jet. Such a strong atmospheric temperature response to absorbing aerosols has been commonly linked to direct solar absorption in the atmosphere (Lau et al., 2006). We demonstrate, however, that changes in the sea surface temperature (SST) gradient and mid-latitude eddies are instrumental in creating a similar deep vertical temperature in response to both types of aerosols, despite the fundamental difference in their forcing structure.

## 2 Methods

### 2.1 The climate model

CESM1 (Community Earth System Model 1) is a coupled ocean–atmosphere–land–sea–ice model. CESM1 climate simulations have been documented extensively (Meehl et al., 2013). The anthropogenic forcing in CESM1 include greenhouse gases (GHGs), as well as prescribed time- and space-evolving concentrations of tropospheric ozone,

stratospheric ozone, the direct effect of sulfate aerosols, and black and primary organic carbon aerosols (Lamarque et al., 2010). The three-mode modal aerosol scheme (MAM3) has been implemented, and it provides internally mixed representations of a number of concentrations and masses. Indirect forcing due to aerosols is included in this model. The present-day emission level of BC is adjusted from the standard model emission inventory to account for potential model underestimation of BC forcing. Our previous analyses (Xu et al., 2013) show that such a correction would improve model-simulated radiative forcing, compared with direct observations. Without the observationally constrained values, the modeled forcing (and simulated temperature change) would be lower by about a factor of two.

## 2.2 Model experiments

- a. Fully coupled model simulations with instantaneous forcing: we used a 394 year, pre-industrial simulation as the control case. Starting from the end of the 319th year, we ran the simulations for 75 years, with the last 60 years of output analyzed, allowing the first 15 years for model spin-up. The forcing is imposed by increasing BC emissions (as a proxy for absorbing aerosols) and SO<sub>2</sub> emissions (a precursor of SO<sub>4</sub>, as a proxy for reflecting aerosols) instantaneously from pre-industrial levels to the present-day level. This methodology is similar to the classical CO<sub>2</sub> doubling experiment (Manabe and Wetherald, 1975). The long averaging time (60 years in the perturbed simulation vs. 394 years for the pre-industrial control simulations) enabled us to dampen the influence of decadal natural variability and to obtain a clear effect due to aerosol perturbation. To increase the signal-to-noise ratio in the BC case (due to smaller BC forcing), five ensembles of perturbed simulations were conducted.
- b. The 20th century transient simulations using fully coupled model simulations, with time-evolving sulfate forcing. The details of the simulations can be found in Meehl et al. (2013).

## Ocean mediation of tropospheric response to reflecting and absorbing aerosols

Y. Xu and S.-P. Xie

Title Page

Abstract

Introduction

Conclusions

References

Tables

Figures

◀

▶

◀

▶

Back

Close

Full Screen / Esc

Printer-friendly Version

Interactive Discussion

- c. The atmospheric-only simulations: the model setting and imposed forcing are identical to (a), but SST is fixed at a pre-industrial level, with only seasonal variability. The model was also run for 75 years.
- d. The SST perturbation experiment: the SST was perturbed with a temperature gradient that increased linearly with latitude, from 0 K at 90° S to 0.5 K at the equator, and then to 1.2 K at 90° N. The values were determined by calculating the SST response to SO<sub>4</sub> in experiment (a). The SST perturbation did not include any longitudinally varying pattern, as our focus here was to understand the zonal averaged temperature response. The perturbed model was run for 25 years (with 10 years of daily output).

### 3 Results and discussions

BC atmospheric radiative forcing is concentrated at 30° N and extends well above the boundary layer to the free atmosphere (Fig. S1 in the Supplement), a structure determined by emission sources and atmospheric concentration. Intuitively, solar absorption by BC results in atmospheric warming. Indeed, BC (Fig. 1 and Fig. S1 for annual mean) induces a warming maximum in the NH mid-latitude troposphere (350 mb, 30 to 40° N), which dwarfs the upper tropical and Arctic warming. This simple thermodynamic mechanism seems consistent with the fact that the magnitude of BC warming is much larger in the boreal summer (JJA) than in the boreal winter (DJF) (1st row in Fig. 1) due to solar insolation.

Interestingly, SO<sub>4</sub> also induces a similar enhanced tropospheric cooling in the mid-latitudes (Figs. 1 and S1 for annual mean). For easy comparison, the response is reversed in sign to be positive. The deep atmospheric response is unexpected from the weak, direct atmospheric forcing of reflecting aerosols (Fig. S1). Also contradictory to the above thermodynamic argument for BC, the temperature response to SO<sub>4</sub> is of a similar magnitude in DJF and JJA.

## Ocean mediation of tropospheric response to reflecting and absorbing aerosols

Y. Xu and S.-P. Xie

Title Page

Abstract

Introduction

Conclusions

References

Tables

Figures

◀

▶

◀

▶

Back

Close

Full Screen / Esc

Printer-friendly Version

Interactive Discussion

The climate response may be decomposed into fast and slow components, defined as the atmospheric response without and due to SST change, respectively (Ganguly et al., 2012). The BC temperature response results predominately from the fast component in the summer due to direct atmospheric heating (Fig. 2), but the slow response dominates in the winter. The  $\text{SO}_4$  fast response, due to the lack of atmospheric forcing, is negligible during summer (except in polar regions where air temperature above sea ice is free to change). The slow response in winter features a narrow maximum around  $30^\circ$  N, and the summer mid-latitude response is weaker and extends into the upper tropics. Therefore, the slow component of the response due to SST change is entirely responsible for the  $\text{SO}_4$  deep atmospheric response and partially responsible for the BC response (Fig. 2).

The dominant role of SST in causing the deep atmospheric response is further confirmed by a set of perturbed-SST experiments, in which the zonal mean SST change in the full  $\text{SO}_4$  simulation is applied to the atmospheric-only model, but with no radiative forcing. The model response to the perturbed SST (3rd row of Fig. 1) is remarkably similar to the  $\text{SO}_4$  slow response (Fig. 2), explaining a large fraction of the total response (2nd row of Fig. 1). The boundary layer air temperature (below 850 mb) is closely tied to the underlying SST because of turbulent mixing, while in the mid-latitudes, the free atmospheric temperature is not tied to the SST because the atmosphere is stably stratified. However, changes in the SST may affect the free troposphere through circulation and eddy adjustments.

The circulation responses to aerosols are shown in the meridional overturning stream function (Fig. 3, positive values indicate clockwise circulation) and zonal averaged zonal wind (Fig. S3, positive values indicate westerly winds). Note that the responses of  $\text{SO}_4$  and BC response are similar, but have opposite signs.  $\text{SO}_4$  cooling in the NH induces an anomalous Hadley cell that rises in the SH and sinks in the NH (Ocko et al., 2014). The atmospheric model forced with  $\text{SO}_4$ -induced SST change largely reproduces the Hadley cell response (3rd row of Fig. 3), highlighting the impor-

tance of the inter-hemispheric SST gradient. Consistent with the Hadley cell response, the NH jet stream shifts equatorward in response to  $\text{SO}_4$  (Fig. S3).

Eddy fluxes are important for maintaining mid-latitude jets. Here, we use the Eliassen–Palm (EP) flux to diagnose the eddy flux adjustment. The EP flux in zonal averaged form was calculated following the method in Holton (1992) using the daily data from the 10 years of control and perturbed SST simulations. The climatology of the EP flux (vector) and EP flux convergence (contour) are shown in Fig. S4a, and are mostly symmetrical between the hemispheres. In climatology, the strong equatorward wave propagation in the mid-latitude troposphere (vectors in Fig. S4a) causes an EP flux divergence (negative value in the dashed contour) that accelerates the westerly wind from  $40\text{--}60^\circ\text{N}$  and maintains the jet stream.

Under the  $\text{SO}_4$ -induced SST perturbation, the EP flux change is strong in the NH mid-latitudes (Fig. 4). Poleward EP flux anomalies reduce the equatorward wave propagation. In the upper troposphere, the EP flux convergence (solid contours) decelerates the vertical mean westerly wind from  $50\text{--}60^\circ\text{N}$ , while the flux divergence (dashed contours) accelerates the vertical mean westerly wind from  $30\text{--}40^\circ\text{N}$ . Thus, westerly winds shift equatorward in response to  $\text{SO}_4$  (Fig. S3). Following the thermal wind relationship (the maximum temperature gradient sets the maximum zonal wind), the equatorward shift of westerly winds must be accompanied by a deep cooling structure (Fig. 1).

Stationary wave activities (Fig. S4b) contribute about 60% of the EP flux change in the NH, with the rest coming from transient eddies. The EP flux change occurs predominately during the winter (about three times larger than the summer change, Fig. S4c) when the background mid-latitude wave activity is strong (Sun et al., 2013). The change in EP flux is consistent with that in the stationary wave refractive index as wave propagation is mainly from a high refractive index region to a low refractive index region (Held and Hou, 1980; Fig. S5).

The quasi-geostrophic refractive index and its change under SST perturbation were calculated following Limpasuvan and Hartmann (2000). In climatology (Fig. S5a), the high refractive index is located in the mid and high latitudes, and the tropics are mainly

## Ocean mediation of tropospheric response to reflecting and absorbing aerosols

Y. Xu and S.-P. Xie

Title Page

Abstract

Introduction

Conclusions

References

Tables

Figures

◀

▶

◀

▶

Back

Close

Full Screen / Esc

Printer-friendly Version

Interactive Discussion

occupied by a smaller refractive index, facilitating the equatorward propagation of mid-latitude wave activities (Sun et al., 2013) (Fig. S4a). The refractive index anomaly due to perturbed SST is mainly at the NH mid-latitude regions (Fig. S5b), which then causes the reduction of wave propagation to the equator (Fig. 4).

The above diagnosis explains the deep tropospheric cooling and associated equatorward shift of the westerly jet in the NH mid-latitudes: (1) the intensified NH Hadley cell accelerates the upper tropospheric westerlies in the subtropics, (2) the EP flux divergence (convergence) accelerates (decelerates) the westerly jet on the equatorward (poleward) flank. Both the Hadley and eddy adjustments are anchored by the SST change with strong meridional gradients. Idealized aqua-planet experiments (Ceppi et al., 2013) exploring the response to a simple mid-latitude heating support the coupled adjustments of the Hadley circulation and mid-latitude jets to realistic aerosol forcing.

## 4 Conclusions

Our results show that despite the fundamental difference in forcing structure, BC and SO<sub>4</sub> share common atmospheric response patterns. The common response is mediated by the ocean through sea-surface temperature gradient, and insensitive to microphysical representations of aerosols. This highlights the importance of ocean-atmosphere interactions in shaping large-scale patterns of climate response, a process overlooked so far in aerosol-climate connection.

The deep mid-latitude warming in response to BC contributes to the retreat of mountain glaciers in the NH near anthropogenic BC emissions, including the Alps (Painter et al., 2013) and Himalayas. Although the cooling effect on the free troposphere is rarely discussed, SO<sub>4</sub> aerosols may have mitigated glacier retreats elsewhere in the past. Into the future, however, more stringent air pollution controls would result in a deep mid-latitude warming, posing a threat to mountain snow packs.

## Ocean mediation of tropospheric response to reflecting and absorbing aerosols

Y. Xu and S.-P. Xie

Title Page

Abstract

Introduction

Conclusions

References

Tables

Figures



Back

Close

Full Screen / Esc

Printer-friendly Version

Interactive Discussion



## Ocean mediation of tropospheric response to reflecting and absorbing aerosols

Y. Xu and S.-P. Xie

Title Page

Abstract

Introduction

Conclusions

References

Tables

Figures



Back

Close

Full Screen / Esc

Printer-friendly Version

Interactive Discussion



The tropospheric temperature and circulation response to  $\text{SO}_4$  is also seen in the 20th century transient simulation (Fig. S2) and the 21st century multi-model projections (Rotstayn et al., 2014). This suggests that the deep temperature structure in the mid-latitudes is a robust feature of aerosol-induced climate change, insensitive to model sub-grid physics. The dynamic response involving the inter-hemispheric Hadley circulation is weak in the case of  $\text{CO}_2$  (Fig. S1) and generally for other hemispherically symmetrical forcing (such as solar and volcanic activities). SST pattern effects have been noted previously (Ramanathan et al., 2005; Xu and Ramanathan, 2010; Friedman et al., 2013; Xie et al., 2013), but our study reveals a fundamental difference in the mid-latitude atmospheric responses to  $\text{CO}_2$  and aerosol forcing. This difference can be exploited to improve the detection and attribution of climate change (Santer et al., 2013). Because aerosol forcing involves stronger mid-latitude storm track adjustments, this result also has important implications for the attribution and projection of extreme events.

**The Supplement related to this article is available online at doi:10.5194/acpd-15-5537-2015-supplement.**

*Acknowledgements.* Y. Xu is supported by the Regional and Global Climate Modeling Program (RGCM) of the US Department of Energy's Office of Science (BER, DE-FC02-97ER62402) and the National Center for Atmospheric Research (NCAR) Advanced Study Programme; and S.-P. Xie by the National Science Foundation (NSF). NCAR is funded by the NSF.

## References

Allen, R. J., Sherwood, S. C., Norris, J. R., and Zender, C. S: Recent Northern Hemisphere tropical expansion primarily driven by black carbon and tropospheric ozone, *Nature*, 485, 350–354, 2012.

**Ocean mediation of tropospheric response to reflecting and absorbing aerosols**

Y. Xu and S.-P. Xie

[Title Page](#)[Abstract](#)[Introduction](#)[Conclusions](#)[References](#)[Tables](#)[Figures](#)[◀](#)[▶](#)[◀](#)[▶](#)[Back](#)[Close](#)[Full Screen / Esc](#)[Printer-friendly Version](#)[Interactive Discussion](#)

- Bollasina, M. A., Ming, Y., and Ramaswamy, V.: Anthropogenic aerosols and the weakening of the South Asian summer monsoon, *Science*, 334, 502–505, 2011.
- Bond, T. C., Doherty, S. J., Fahey, D. W., Forster, P. M., Berntsen, T., Deangelo, B. J., Flanner, M. G., Ghan, S., Kärcher, B., Koch, D., Kinne, S., Kondo, Y., Quinn, P. K., Sarofim, M. C., Schultz, M. G., Schulz, M., Venkataraman, C., Zhang, H., Zhang, S., Bellouin, N., Guttikunda, S. K., Hopke, P. K., Jacobson, M. Z., Kaiser, J. W., Klimont, Z., Lohmann, U., Schwarz, J. P., Shindell, D., Storelvmo, T., Warren, S. G., and Zender, C. S.: Bounding the role of black carbon in the climate system: A scientific assessment, *J. Geophys. Res. Atmos.*, 118, 5380–5552, 2013.
- Ceppi, P., Hwang, Y.-T., Liu, X., Frierson, D. M. W., and Hartmann, D. L.: The relationship between the ITCZ and the Southern Hemispheric eddy-driven jet, *J. Geophys. Res.-Atmos.*, 118, 5136–5146, 2013.
- Friedman, A. R., Hwang, Y.-T., Chiang, J. C. H., and Frierson, D. M. W.: Interhemispheric temperature asymmetry over the 20th century and in future projections, *J. Clim.*, 26, 5419–5433, 2013.
- Ganguly, D., Rasch, P. J., Wang, H., and Yoon, J.: Fast and slow responses of the South Asian monsoon system to anthropogenic aerosols, *Geophys. Res. Lett.*, 39, L18804, doi:10.1029/2012GL053043, 2012.
- Held, I. M. and Hou, A. Y.: Nonlinear axially symmetric circulations in a nearly inviscid atmosphere, *J. Atmos. Sci.*, 37, 515–533, 1980.
- Holton, J.: *An Introduction to Dynamic Meteorology*, 3rd Edition, Academic Press, San Diego, 511 pp., 1992.
- Hwang, Y.-T., Frierson, D. M. W., and Kang, S. M.: Anthropogenic sulfate aerosol and the southward shift of tropical precipitation in the late 20th century, *Geophys. Res. Lett.*, 40, 2845–2850, 2013.
- Koch, D. and Del Genio, A. D.: Black carbon semi-direct effects on cloud cover: review and synthesis, *Atmos. Chem. Phys.*, 10, 7685–7696, doi:10.5194/acp-10-7685-2010, 2010.
- Lamarque, J.-F., Bond, T. C., Eyring, V., Granier, C., Heil, A., Klimont, Z., Lee, D., Liousse, C., Mieville, A., Owen, B., Schultz M. G., Shindell, D., Smith, S. J., Stehfest, E., Van Aardenne, J., Cooper, O. R., Kainuma, M., Mahowald, N., McConnell, J. R., Naik, V., Riahi, K., and van Vuuren, D. P.: Historical (1850–2000) gridded anthropogenic and biomass burning emissions of reactive gases and aerosols: methodology and application, *Atmos. Chem. Phys.*, 10, 7017–7039, doi:10.5194/acp-10-7017-2010, 2010.



## Ocean mediation of tropospheric response to reflecting and absorbing aerosols

Y. Xu and S.-P. Xie

Title Page

Abstract

Introduction

Conclusions

References

Tables

Figures

◀

▶

◀

▶

Back

Close

Full Screen / Esc

Printer-friendly Version

Interactive Discussion

- Santer, B. D., Painter, J. F., Mears, C. a., Doutriaux, C., Caldwell, P., Arblaster, J. M., Cameron-Smith, P. J., Gillett, N. P., Gleckler, P. J., Lanzante, J., Perlwitz, J., Solomon, S., Stott, P. a., Taylor, K. E., Terray, L., Thorne, P. W., Wehner, M. F., Wentz, F. J., Wigley, T. M. L., Wilcox, L. J., and Zou, C.-Z.: Identifying human influences on atmospheric temperature, *P. Natl. Acad. Sci.*, 110, 26–33, 2013.
- Shindell, D. T., Voulgarakis, A., Faluvegi, G., and Milly, G.: Precipitation response to regional radiative forcing, *Atmos. Chem. Phys.*, 12, 6969–6982, doi:10.5194/acp-12-6969-2012, 2012.
- Smith, S. J., van Aardenne, J., Klimont, Z., Andres, R. J., Volke, A., and Delgado Arias, S.: Anthropogenic sulfur dioxide emissions: 1850–2005, *Atmos. Chem. Phys.*, 11, 1101–1116, doi:10.5194/acp-11-1101-2011, 2011.
- Sun, L., Chen, G., and Lu, J.: Sensitivities and mechanisms of the zonal mean atmospheric circulation response to tropical warming, *J. Atmos. Sci.*, 70, 2487–2504, 2013.
- Vinoj, V., Rasch, P. J., Wang, H., Yoon, J.-H., Ma, P.-L., Landu, K., and Singh, B.: Short-term modulation of Indian summer monsoon rainfall by West Asian dust, *Nat. Geosci.*, 7, 308–313, 2014.
- Xie, S., Lu, B., and Xiang, B.: Similar spatial patterns of climate responses to aerosol and greenhouse gas changes, *Nat. Geosci.*, 6, 828–832, 2013.
- Xu, Y. and Ramanathan, V.: Latitudinally asymmetric response of global surface temperature: implications for regional climate change, *Geophys. Res. Lett.*, 39, L13706, doi:10.1029/2012GL052116, 2012.
- Xu, Y., Bahadur, R., Zhao, C., and Ruby Leung, L.: Estimating the radiative forcing of carbonaceous aerosols over California based on satellite and ground observations, *J. Geophys. Res.-Atmos.*, 118, 11148–11160, 2013.

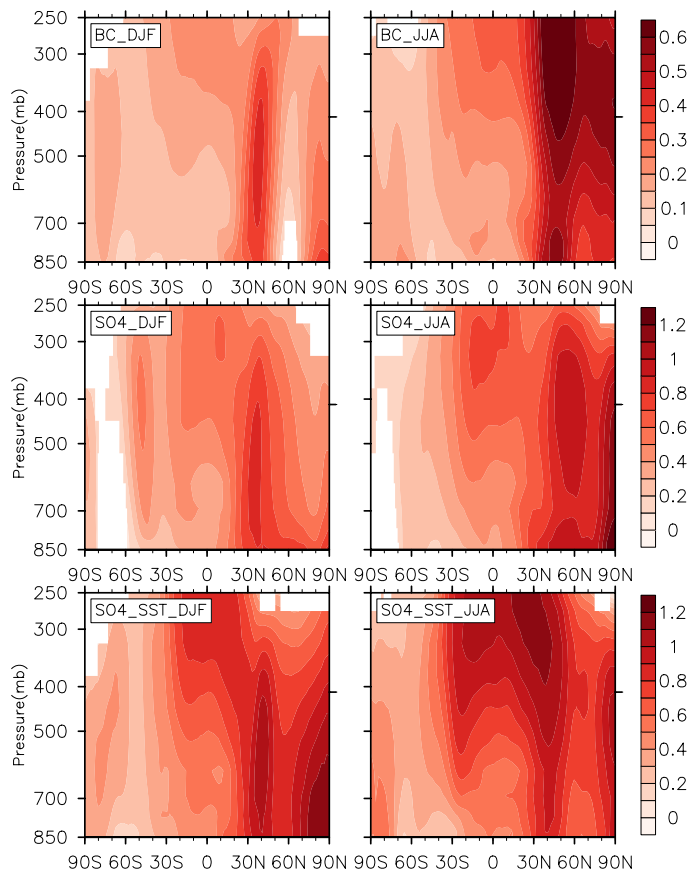


**Figure 1.** Temperature response (K) as a function of latitude and pressure to BC (1st row),  $\text{SO}_4$  (2nd row), and  $\text{SO}_4$ -induced SST perturbation ( $\text{SO}_4\text{-SST}$ ) (3rd row). Note that the  $\text{SO}_4$  and  $\text{SO}_4\text{-SST}$  response are of the opposite sign. The color scale is chosen considering that the top-of-atmosphere forcing of  $\text{SO}_4$  is about twice that of BC in this model. The left and right columns are the DJF and JJA average, respectively.

**Ocean mediation of tropospheric response to reflecting and absorbing aerosols**

Y. Xu and S.-P. Xie

Title Page

Abstract Introduction

Conclusions References

Tables Figures

◀ ▶

◀ ▶

Back Close

Full Screen / Esc

Printer-friendly Version

Interactive Discussion



## Ocean mediation of tropospheric response to reflecting and absorbing aerosols

Y. Xu and S.-P. Xie

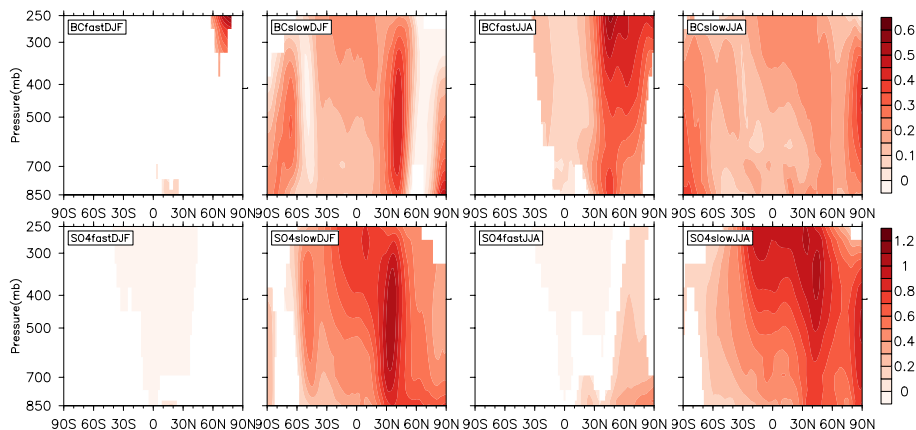


**Figure 2.** Similar to Fig. 1, but for fast (1st and 3rd column) and slow components (2nd and 4th column) temperature response (in K). The fast component is calculated by running an atmospheric-only simulation with changed atmospheric compositions, but fixed SST, while the slow component is the difference between the total (Fig. 1) and fast responses.

Title Page

Abstract

Introduction

Conclusions

References

Tables

Figures

◀

▶

◀

▶

Back

Close

Full Screen / Esc

Printer-friendly Version

Interactive Discussion



## Ocean mediation of tropospheric response to reflecting and absorbing aerosols

Y. Xu and S.-P. Xie

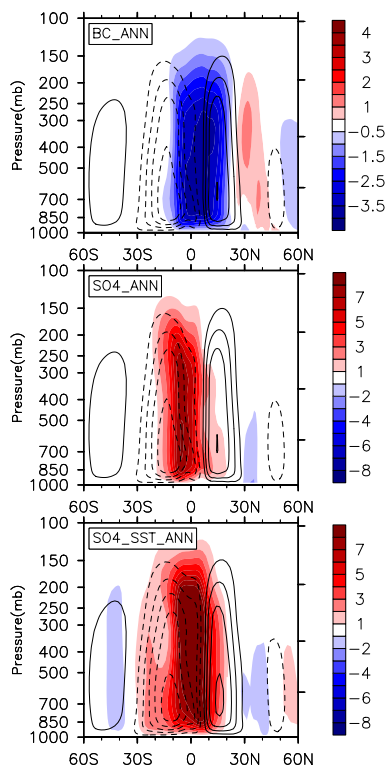


**Figure 3.** Zonal mean meridional stream function change ( $10^9 \text{ kg s}^{-1}$ ), in response to BC (1st row),  $\text{SO}_4$  (2nd row), and  $\text{SO}_4$ -induced SST perturbation ( $\text{SO}_4\text{-SST}$ ) (3rd row). Climatological stream function is shown in contour lines with an interval of 40. The negative values (blue shading and dashed lines) of the stream function indicate that the meridional flow is counter-clockwise.

[Title Page](#)[Abstract](#)[Introduction](#)[Conclusions](#)[References](#)[Tables](#)[Figures](#)[◀](#)[▶](#)[◀](#)[▶](#)[Back](#)[Close](#)[Full Screen / Esc](#)[Printer-friendly Version](#)[Interactive Discussion](#)

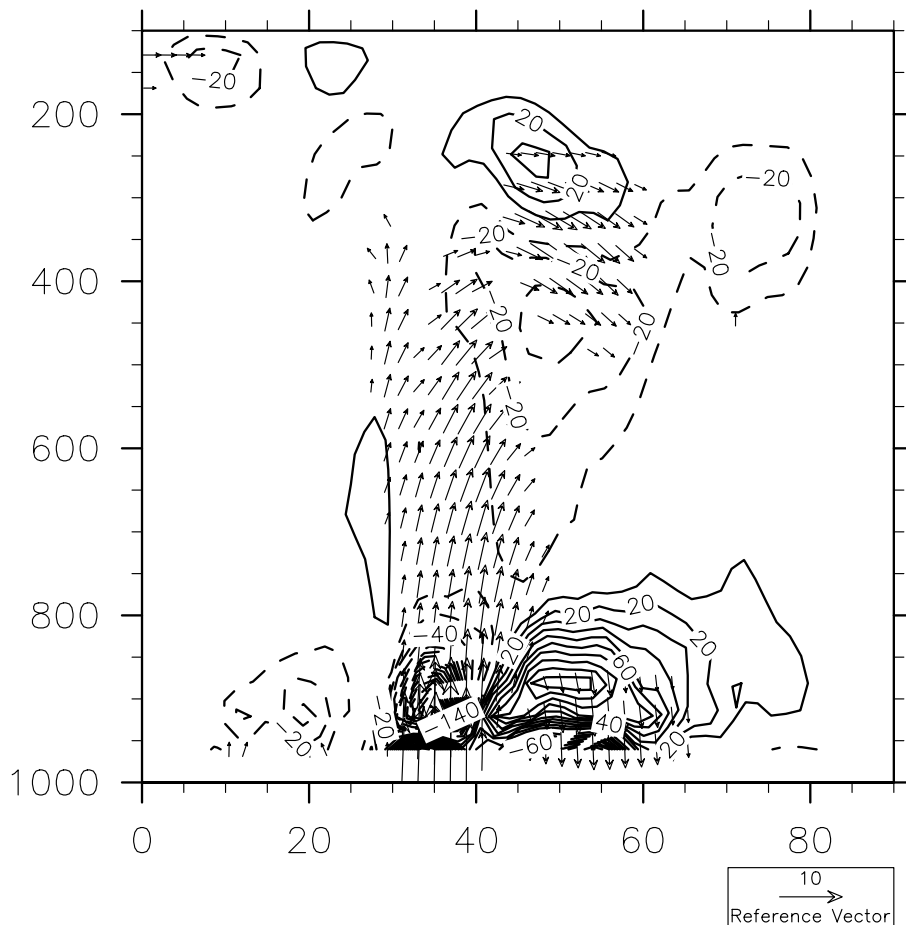


**Figure 4.** Eliassen–Palm (EP) flux change due to  $\text{SO}_4$ -induced SST perturbation ( $\text{SO}_4\text{-SST}$ ). The convergence (solid contours) and divergence (dashed contours) of the EP flux correspond to a deceleration and acceleration of the westerly mean flow, respectively.